Temperature dependence of the InP band gap from a photoluminescence study

L. Pavesi and F. Piazza
Dipartimento di Fisica, Università di Trento, I-38050 Povo (Trento), Italy

A. Rudra, J. F. Carlin, and M. Ilegems
Institut de Micro et Optoélectronique, Ecole Polytechnique Fédérale, CH-1015 Lausanne, Switzerland
(Received 20 March 1991)

A set of parameters for the temperature dependence of the direct band gap of InP has been determined by fitting the excitonic recombination energy in the photoluminescence (PL) spectra between 2 and 250 K. We have used high-quality InP samples grown by chemical beam epitaxy. The superfluid-helium temperature PL spectra are characterized by strong excitonic transitions (the excited state n=2 of the exciton is observed too) from which we have determined the binding energy of the exciton (E_b=5.3 meV) and the band-gap energy (E_g=1.4239 eV at 1.3 K). The variable-temperature PL spectra are characterized by excitonic transitions for temperatures as high as 250 K. The expression $E_g(T) = 1.4539 - 0.0359(1 + 2/\{\exp[209/T\ (\mathrm{K})] - 1\})$ eV, which extrapolates to E_g=1.347 eV at 300 K, is proposed for the temperature dependence of the InP band gap over the temperature range 0–300 K.

InP is a III-V semiconductor that is a key material in the modern optoelectronic industry.[1] However, the growth of good quality samples of InP has posed several problems in the past.[1] Because of these, some important physical parameters of this semiconductor have not yet been determined with sufficient precision. In particular, different values of the direct band gap (E_g) are reported in the literature (see Fig. 1) and the temperature dependence of E_g is still an open question.[2–4]

In 1964, Turner, Reese, and Petit[5] measured the absorption and emission spectra of InP as a function of the temperature. Subsequently Varshni[2] fitted their experimental data with the following empirical formula for $E_g(T)$:

$$E_g(T) = E_g(0) - \alpha T^2/(\beta + T), \tag{1}$$

where β is proportional to the Debye temperature Θ_D, $\beta \simeq 3/8\Theta_D$ for temperatures higher than Θ_D.[6] The low-temperature dependence is therefore quadratic in T, and it is due to the electron-phonon interaction. The two parameters in Eq. (1) have no clear physical significance for low temperatures. The Varshni parameters for InP are given in Table I.

Equation (1) has been used until now to describe the band-gap dependence on the temperature for almost all the III-V semiconductors. Subsequently, an additional phenomenological expression has been proposed to describe the thermal band-gap shrinkage.[7] This model considers the renormalization of electronic states due to the interaction with phonons with an average phonon frequency. Hence the expression contains a Bose-Einstein statistical factor:

$$E_g(T) = E_B - a_B(1 + \{2[\exp(\Theta/T) - 1]\}), \tag{2}$$

where Θ is related to the average phonon frequency and a_B describes the strength of the interaction.

The main difference between Eqs. (1) and (2) is in the low-temperature region where the quadratic dependence of Eq. (1) is replaced by an exponential dependence in Eq. (2). The high-temperature trend, instead, is linear both in Eq. (1) and in Eq. (2). In Ref. 6 it has been demonstrated that the dynamic part of the band-gap energy shift is described by the Bose-Einstein relation whereas the Varshni equation is a second-order approximation to the Bose-Einstein relation valid for $\Theta \ll T$.

Very recently two papers have addressed the problem of the determination of $E_g(T)$ in InP.[3,4] In one paper,[3] the ellipsometry technique has been used in order to measure not only the direct fundamental gap, but also higher-energy transitions as $E_1, E_0 + \Delta'$, etc. In the other,[4] the photoreflectance method has been used and the same quantities have been measured. The conclusions are in contrast with two different temperature dependences for

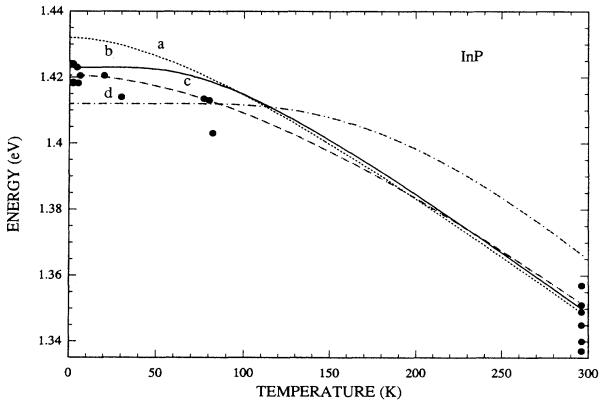

FIG. 1. Experimental data (disk) for the energy gap of InP reported in the collection of data given in Ref. 3 at different temperatures. The lines are the temperature dependence of the energy gap as proposed in Ref. 4 [curve (*a*) using Eq. (1) and curve (*b*) using Eq. (2)], in Ref. 2 [curve (*c*)] and in Ref. 3 [curve (*d*)].

TABLE I. Values of the parameters for the energy dependence of the energy gap of InP. The meaning of the different symbols is given in the text. (The numbers in parentheses represent a 95% confidence interval.)

$E_g(0)$ (eV)	α (meV/K)	β (K)	Validity range (K)	
1.424±0.005	1.02±3	823±200	0-250	this work
1.432±0.007	0.41±0.03	136±60	77-870	Ref. 4
1.4206	0.49	327	0-300	Ref. 2
E_B (eV)	a_B (meV)	Θ_B (K)	Validity range (K)	
1.4539±0.002	35.9±1.2	209±9	0–250	this work
1.474±0.010	51±2	259±10	77–870	Ref. 4
1.629(111)	217(113)	697(117)	30–420	Ref. 3

E_g (see Fig. 1 and Table I).

The recent improvement in the crystal growth technique allows the growth of samples with a very low density of residual impurity and with very low compensation ratio.[8-10] These samples are characterized by low-temperature photoluminescence spectra dominated by intrinsic transitions. Thus it is possible to monitor the band-gap energy as a function of the temperature by measuring the photoluminescence spectrum.[11] This method is more direct than ellipsometry or photoreflectance, although it can be used only for E_g.

In this paper we report on variable temperature photoluminescence of very-high-quality InP samples grown by chemical beam epitaxy in order to measure $E_g(T)$ accurately. The main electrical properties of the samples are given in Table II. More details about the growth have been already published in Ref. 10.

The experimental setup for the photoluminescence measurements is composed of a double monochromator followed by a photomultiplier tube with a GaAs photocathode. The 632.8-nm line of a He-Ne laser serves as excitation source. The samples are positioned in a liquid-bath cryostat and a carbon glass resistance soldered on the sample holder serves as a temperature sensor and drives a heating resistor through a feedback circuit. The precision on the temperature stabilization is about 0.1 K for temperatures up to 30 K and about 2 K for higher temperatures.

Figure 2 shows low-temperature photoluminescence (PL) spectra of samples No. 3 and No. 2.[12-15] In part (a) the main features are the free exciton recombination line ($X_{n=1}$), the transitions associated with the different rotational states of the complex formed by an exciton bound to a neutral donor $(D^0X)_n$ with n up to 5, the recombination of a free hole with an electron bound to a donor (D^0h), the recombination of an exciton bound to an ionized donor (D^+X), and the low-energy doublet due

TABLE II. Growth parameters and electrical characteristics of the samples studied. T_s is the substrate temperature during the growth, T_P is the cracking temperature of the PH_3 gas, N_D-N_A is the residual doping level, $\mu_{77\,K}$ is the 77-K mobility, and d is the layer thickness.

	No. 1	No. 2	No. 3
T_S (°C)	520	540	540
T_P (°C)	885	885	760
$N_D - N_A$ (10^{14} cm^{-3})	15	4.1	1.3
$\mu_{77\,K}$ (cm^2 V^{-1} s^{-1})	51 000	113 000	176 000
d (μm)	2	7	5.5

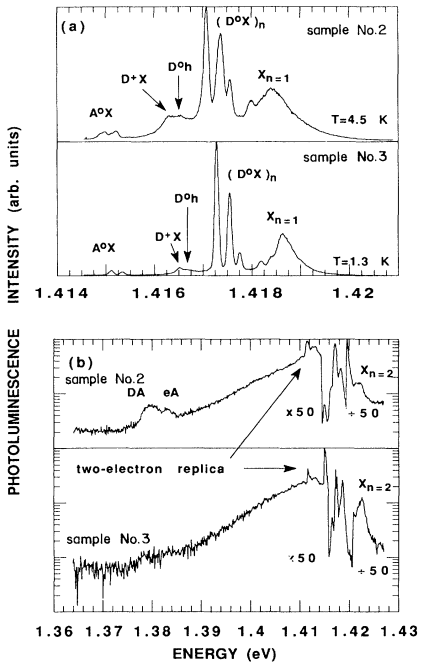

FIG. 2. Low-temperature photoluminescence spectra of InP. (a) shows the excitonic region for sample No. 2 (upper curve) and for sample No. 3 (lower curve). (b) reports the PL spectra on a logarithmic intensity scale of the same samples in a wider energy region. In the excitonic region the luminescence intensity has been attenuated by a factor of 50 in order to avoid saturation of the phototube. The labels on the spectra have the following meaning: $X_{n=1}$ exciton recombination, D^0X exciton bound to a neutral donor recombination, D^0h free hole to a donor bound electron transition, A^0X exciton bound to a neutral acceptor recombination, DA donor to acceptor pair transition, eA free electron to a hole bound to a neutral acceptor recombination. The laser excitation intensity is 60 mW cm^{-2} for all the spectra except for sample No. 2 in (a) where an excitation intensity of 600 mW cm^{-2} has been used.

to the recombination of an exciton bound to an acceptor (A^0X). Both samples show similar luminescence spectra. However, the relative intensities of the PL emission bands are different in the two samples due to a higher donor concentration and to a larger compensation ratio for sample No. 2 than for sample No. 3 (see Table II). Also a small energy shift between the spectral peak positions is evident. This fact is usually found in the literature (see Table III) and may be due to residual strain or local field effects.

Figure 2(b) shows the PL spectra of the same samples taken in a larger energy interval. At high energies the recombination of the first excited state of the exciton ($X_{n=2}$) is visible; at about 1.412 eV we observe the structured emission from two electron satellites of the $(D^0X)_n$ lines. In sample No. 2, a band due to the superposition of the donor-to-acceptor (DA) recombination and to the recombination of a free electron with a hole bound to an acceptor (eA) is present at about 1.38 eV. The acceptor involved is carbon.[15] This band is absent or has a very low intensity for sample No. 3 in agreement with the results of electrical measurements which indicates a lower compensation in sample No. 3 (see Table II).

Table III reports the energy positions of some PL features for sample No. 3 and a comparison with the data in the literature.[12,8] Using $E_b = \frac{4}{3}[\hbar\omega(2s) - \hbar\omega(1s)]$ for the excitonic binding energy, we find $E_b \simeq 5.3$ meV which has to be compared with the effective mass value of 5.14–5.17 meV.[14] Hence from the position of the $n=1$ exciton recombination line we find an energy gap of 1.4239 eV at 1.3 K. The binding energy of the donor deduced from the data is equal to 7.2 meV in good agreement with the prediction of the effective-mass approximation which gives a value of 7.14 meV.[15]

The PL spectra of sample No. 3 is reported in Fig. 3 for different temperatures. As T is raised the high-energy features increase in relative intensity with respect to the bound exciton recombinations. The A^0X line disappears from the spectra for $T \simeq 12$ K and the $(D^0X)_n$ lines for $T \simeq 30$ K, while the D^0h line is still observable as a small low-energy shoulder on the main peak up to $T \simeq 83$ K. As the temperature is increased further, the intensity of the (e-h) band emission increases and eventually, for $T \geq 120$ K, dominates the spectrum. However, the $n=1$ excitonic recombination line remains clearly observable up to $T \simeq 250$ K (not shown in the figure). The persistence of the excitonic transition up to high temperature has been also indirectly observed in Ref. 4. In fact, to extract reliable information from the photoreflectance data a line-shape procedure which includes excitonic effects up to room temperature has been used in Ref. 4.

A fit to the PL line shape has been performed and the different contributions (excitonic and free electron-hole pair recombinations) are indicated in Fig. 3 as solid lines for the $T=83$ K spectrum. The luminescence line shape and fitting procedure are described in Ref. 11. The band gap position has been obtained by subtracting E_b from the peak energy position, i.e., E_g is not an adjustable parameter. The resulting line shape reproduces quite well the experimental data. This fit confirms the attribution of the main peak to the exciton recombination and shows the importance of the recombination of excited excitonic states. The (e-h) emission band is pretty well reproduced supporting the procedure we used to extract E_g from the experimental data.

Figure 4 shows the energy gap as a function of the temperature obtained by subtracting E_b from the energy of the PL excitonic recombination lines. The use of a temperature-independent excitonic binding energy is necessary due to the scarce knowledge of the InP parameters and introduces an uncertainty of the order of 1 meV on the energy gap values.[15] A least-squares fit to

TABLE III. Low-temperature energy values for the excitonic $n=1$ and $n=2$ recombination lines [$\hbar\omega(n=1)$ and $\hbar\omega(n=2)$, respectively], the hole to donor recombination [$\hbar\omega(D^0h)$], the direct energy gap (E_g), the excitonic binding energy (E_b), and the donor binding energy (E_d). All the data are in eV.

	This work	Ref. 8	Ref. 13
$\hbar\omega(1s)$	1.4186	1.4188	1.4183
$\hbar\omega(2s)$	1.4226		
$\hbar\omega(D^0h)$	1.4166	1.4168	1.4163
E_g	1.4239		1.4237
E_b	0.0053		0.0054
E_d	0.0072		0.0074

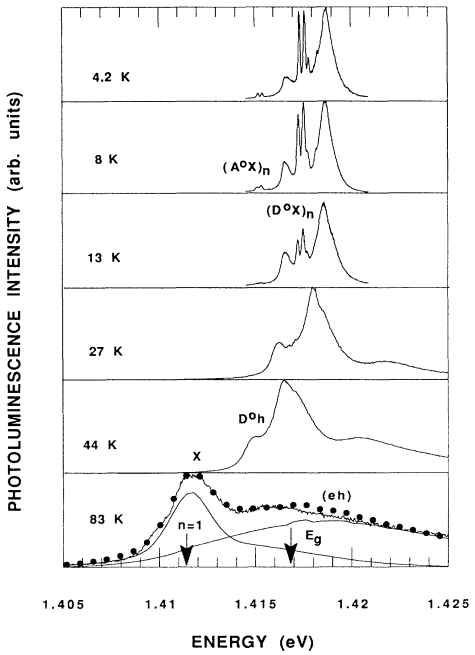

FIG. 3. Photoluminescence spectra of sample No. 3 at different sample temperatures, T. The labels on the spectra have the same meaning as in Fig. 2. The spectrum at $T=83$ K has been fitted by a line-shape theory with the following fitting parameters: excitonic broadening 2.5 meV, broadening of the continuum states 10.6 meV, ratio between free to bound contributions 0.3. The solid lines represent the excitonic and the continuum contribution to the line shape. The sum of the two contributions, i.e., the total line-shape intensity, is shown by the small disk. Also indicated are the energy position of the $n=1$ exciton resonance and the energy gap value at 83 K.

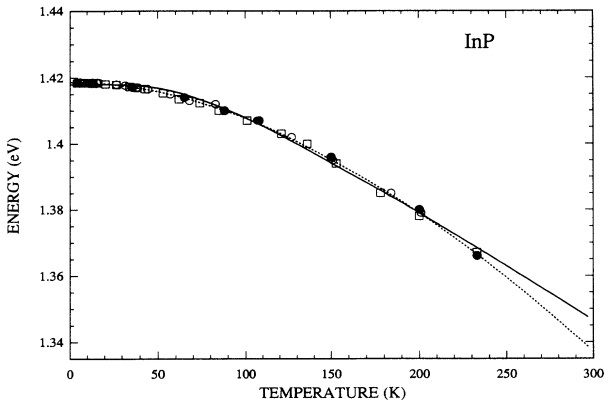

FIG. 4. Temperature dependence of the energy gap (E_g) extracted from the experimental data. The different symbols refer to the three samples investigated: disk No. 1, open square, No. 2, and open circle, No. 3. The lines are the resulting temperature dependence of E_g obtained by a least-square fit to the Varshni equation [Eq. (1), dotted line] and to the Bose-Einstein expression [eq. (2), full line]. The fitting parameters are given in Table I.

the experimental data from three different samples with Eqs. (1) and (2) yields the parameters reported in Table I. The errors on the parameters are also given in the table.

The best fit is obtained using Varshni's equation [Eq. 1)], but the resulting expression does not extrapolate to the high-temperature data reported in the literature.[4] Inversely, a Varshni fit to these high-temperature data leads to an $E_g(T)$ expression which overevaluates the low-temperature band gap reported by most workers (Fig. 1). This might be understood as follows: the temperature interval up to 250 K is dominated by the dynamic part of the electron-phonon interaction which in the Varshni equation is given by the quadratic dependence and, consequently, the fit gives a large value for β. This clearly means that the α and β parameters determined in this study are relevant only up to 250 K. The large values of uncertainty on both α and β indicate the presence of a correlation between these two parameters.

On the other hand, the fit by the Bose-Einstein expression [Eq. (2)] is of good quality and can be made to fit also the high-temperature data. The resulting mean phonon frequency is $\hbar\omega_{ph} \simeq 18$ meV which compares very well with the mean frequency of the entire phonon spectrum of $\simeq 20$ meV.[15] These facts suggest that for practical use Eq. (1) with the parameters given in Table I is valuable for temperatures up to 250 K and expression (2) for a wider temperature interval. As an example, using relation (2) with the newly determined parameters, the room-temperature band-gap energy is $E_g(300\ \text{K})=1.347$ eV at 300 K.

The discrepancy with the earlier measurements[5,2] may be due to the fact that the original parameters of Varshni are based on data extracted by PL measurements on samples of low quality (compare the PL spectra). A systematic shift of about 4 meV exists between our data and the data reported in Ref. 5 which could be due to the wrong identification of a (hD^0) transition as the excitonic one. On the other hand, the fits reported in Ref. 4 are based on high-temperature measurements. The agreement with our $E_g(T)$ is indeed good at high temperature. At low temperature the three expressions are somehow different with the data of Hang, Shen, and Pollack at higher energy than ours. For example, $E_g(0\ \text{K})=1.432$ eV (Ref. 4) while $E_g(0\ \text{K})=1.424$ eV in our work. Finally, we note that the disagreement with the findings of Ref. 3 is rather important. It is worth noting that the ellipsometry technique is sensible to the state of the surface (oxide formation) and that it is very suitable to measure the high-energy transitions with a large oscillator strength but it is not very precise in the measure of E_g due to the small resonance associated with the fundamental gap.[3]

In conclusion, via variable temperature photoluminescence experiments, we have been able to extract a highly reliable expression for the energy gap dependence on the temperature. Our results point to a great contribution of the dynamical electron-phonon interaction to $E_g(T)$ for $T \leq 300$ K.

We acknowledge the technical assistance of F. Rossi and O. Pilla.

[1] *GaInAsP Alloy semiconductors*, edited by T. P. Pearsall (Wiley, Chichester, 1982); M. Razeghi, in *The MOCVD Challenge* (Hilger, Bristol, 1989), Vol. 1.
[2] Y. P. Varshni, Physica (Amsterdam) **34**, 149 (1967).
[3] P. Lautenschlager *et al.* Phys. Rev. B **36**, 4813 (1987).
[4] Z. Hang *et al.* Solid State Commun. **73**, 15 (1990).
[5] W. J. Turner *et al.* Phys. Rev. **136**, A1467 (1964).
[6] A. Manoogian and J.C. Wooley, Can. J. Phys. **62**, 285 (1984).
[7] M. Cardona and S. Gopalan, in *Progress in Electron Properties of Solids*, edited by E. Doni *et al.* (Kluwer Academic, Dordrecht, 1989), p. 51.
[8] M. Razeghi *et al.* Appl. Phys. Lett. **52**, 117 (1988).
[9] H. Heinecke *et al.* Electron. Lett. **26**, 213 (1990).
[10] A. Rudra *et al.* J. Cryst. Growth **111**, 589 (1991).
[11] M. Guzzi *et al.* (unpublished). For the line-shape theory see also L. Pavesi *et al.* J. Phys. C **21**, 1485 (1988).
[12] W. Rühle and W. Klingenstein, Phys. Rev. B **18**, 7011 (1978).
[13] P. J. Dean and M. S. Skolnick, J. Appl. Phys. **54**, 346 (1982).
[14] A. Baldereschi and N. C. Lipari, Phys. Rev. B **3**, 439 (1971).
[15] *Numerical Data and Functional Relationships in Science and Technology*, edited G. Harbeke *et al.* Landolt-Börnstein, New Series, Vol. 17a (Springer-Verlag, Berlin, 1987), p. 281.